Multiscale analysis of woven composites - scale transition via macroelement

M. Wierer, M. Šejnoha* and J. Zeman

Submitted for review in the Building research journal, 07/04/05

Abstract

The multiscale analysis has become a common tool in the study of many complicated structures such as composites. In this regard, two possible modeling strategies, so called coupled and uncoupled approaches, are available. While the uncoupled approach treats individual scales separately and thus divides the analysis typically into two or three mutually independent steps, the coupled approach allows combining analyses at all scales in a common framework. Clearly, formulation of a macroelement belongs to the group of coupled approaches. It starts from meshing the micro or mesostructure into a net of finite elements with associated global stiffness matrix. All inner degrees of freedom (dofs) of the finite element mesh are then condensed out together with applying certain multipoint constraints to unwanted boundary degrees of freedom. The resulting macroelement stiffness matrix establishes the scale to scale interface (micro-meso, meso-macro). This approach is introduced here in conjunction with the analysis of complex wound composite tubes. A number of numerical examples are presented to support applicability of the proposed approach.

1 Introduction

Undoubtable benefits offered by composite materials such as high strength, light weight, non-corrosive properties, etc., have recently attracted many design engineers in the civil engineering industry, primarily in conjunction with rehabilitation and repair of concrete and masonry structures. A lucid discussion on this subject is given in (Šejnoha, 1999).

It is a well-understood and widely accepted fact that an overall response of composite structures is highly influenced both by the material behavior and geometrical arrangement of distinct phases of the composite system. Such a research venture inevitably calls for analyses on different length scales. However, each scale of modeling is typically several orders of magnitude smaller that the preceding one, which makes the direct "brute force" approach, relying on detailed description of the whole structure with all details present, practically intractable even on modern powerful computers. Therefore, to obtain a realistic prediction of the behavior of the whole structure, a suitable method of attack that

*Faculty of Civil Engineering, CTU in Prague; Thákurova 7, 166 29 Prague 6; tel.:+420224354494; e-mail: sejnom@fsv.cvut.cz

efficiently combines the analysis on individual scales of the structure, is needed. Thus the solution strategies based on multiscale analysis appear as a natural choice, see, e.g., (Fish, 1992; Fish et al., 1997, 1999; Kouznetsova et al., 2002). General overview of various multiscale techniques can also be found in (Zeman, 2003; Wierer, 2005). Regardless of the method used, it is clear that a reliable transfer of required information between various modeling levels is crucial for the success of the selected method.

Various multi-scale computational techniques available in the literature can be included in the following categories:

1. Multiple scale expansion methods - These methods are sometimes called uncoupled. Generally, they are based on the separate homogenization at individual modeling levels and the results from lower level are used as an input for the analysis on higher level.

2. Superposition based methods (coupled approach) - Contrary to uncoupled methods the coupled approaches build on mutually dependent homogenization on individual scales. As such, this approach can include nonlinear behavior including failure analysis on every scale much easily compared to uncoupled problem.

The approach based on the formulation of a certain macroelement, successfully used in the analysis of textile composites (Whitcomb et al., 1994), fits well within the framework of coupled methods. In the present vocabulary, the construction of such element combines static condensation and application of multipoint constrains resulting in a global macroelement stiffness matrix directly applicable in the macroscopic analysis.

The benefits of this method can be well appreciated in the case of woven composites, where the difference between individual scales is relatively small so that the classical homogenization techniques, which draw on the existence of macroscopically uniform stress and strain fields over a sufficiently large portion of meso (micro) geometry, cannot be involved. Homogenization of such material systems is also the main objective of the present contribution.

The paper is divided as follows. The theoretical background for the present approach is outlined in the first section. The next section reviews essential steps of the use of macroelement in coupled multiscale analysis. Several numerical examples are offered in Section 4 to show both advantages and disadvantages of the suggested approach when applied to the multiscale modeling of woven composites. Although the proposed approach is applicable for coupling of any adjacent scales, we limit our attention to two-scale composite with a well defined geometry on mesoscale, Fig. 1. Thus only the transition from meso to macroscale is assumed throughout the remaining part of this paper.

2 Theoretical background

Recently, continuum elements have been developed to account for a textile and woven type microstructure within a single element. For more details see (Foye, 1988; Woo and Whitcomb, 1992). The elements described in these references are based on a single assumed displacement field throughout the entire element. A more general element formulation that includes the single field approximation as a degenerate state is presented

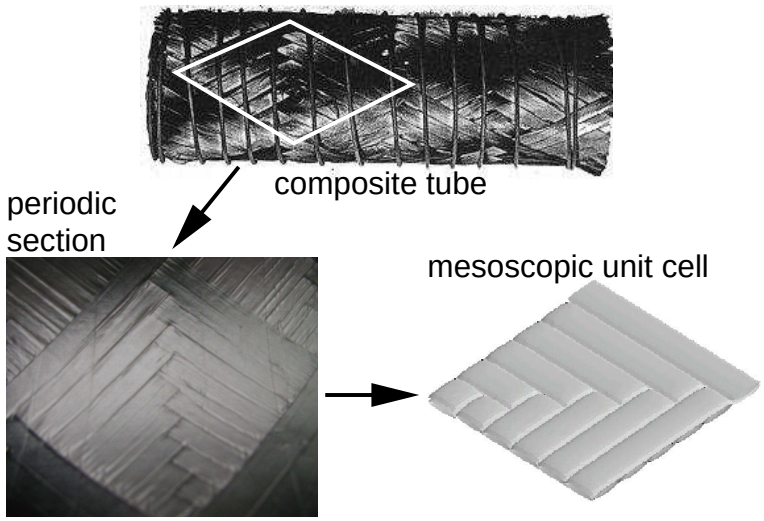

Figure 1: Wound composite tube on macroscale and mesoscopic unit cell

herein. This formulation is an example of element reduced substructuring (Kamel et al., 1972).

In brief, the implementation starts from the development of an ordinary finite element mesh for a certain mesoscopic unit cell (MUC). Such MUC often arises from the periodic character of the composite geometry, Fig. 1. In the next step, the interior degrees of freedom are statically condensed out. Next, a number and locations of the desired boundary degrees of freedom are selected. Finally, the original boundary degrees of freedom are expressed in terms of the selected boundary degrees of freedom linked to so called master nodes.

To illustrate the process of substructuring, consider, as an example, a mesoscopic finite element mesh in Fig. 2. Assume that the governing equations are partitioned as follows

$$\begin{pmatrix} \boldsymbol{K}_{AA} & \boldsymbol{K}_{AB} \\ \boldsymbol{K}_{BA} & \boldsymbol{K}_{BB} \end{pmatrix} \begin{pmatrix} \mathbf{q}_A \\ \mathbf{q}_B \end{pmatrix} = \begin{pmatrix} \mathbf{F}_A \\ \mathbf{F}_B \end{pmatrix}, \tag{1}$$

where $\boldsymbol{K}_{XX}$ are submatrices of the global stiffness matrix, $\mathbf{F}_X$ are nodal forces, $\mathbf{q}_A$ is the vector of unknowns to be condensed out and $\mathbf{q}_B$ are unknowns, which will remain. The resulting reduced stiffness matrix and the corresponding load vector assume the form

$$\overline{\boldsymbol{K}}_{BB} = \boldsymbol{K}_{BB} - \boldsymbol{K}_{AA}^{-1}\boldsymbol{K}_{AB} \tag{2}$$

$$\overline{\mathbf{F}}_B = \mathbf{F}_B - \boldsymbol{K}_{AB}^{\top}\boldsymbol{K}_{AA}^{-1}\mathbf{F}_A. \tag{3}$$

This procedure is often not practical owing to large matrix multiplications as a consequence of matrix inversion that destroys the sparsity in $\boldsymbol{K}_{AA}$. The elimination of internal degrees of freedom, however, can be also accomplished using the Gauss elimination if the degrees of freedom to be eliminated are grouped together either at the beginning or at the end of the list of unknowns. To that end, assume that the degrees of freedom to be eliminated (the number is n_A) are stored at the beginning of the list of unknowns. The direct Gauss elimination procedure is then applied to n_A columns (i.e., removing n_A columns). In summary, this procedure reads:

1. For $i = 1$ to n_A begin:

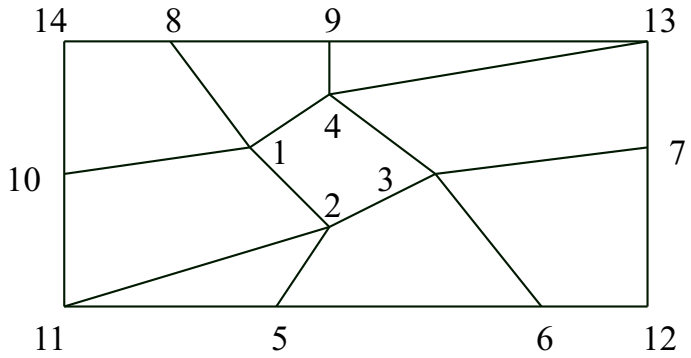

Figure 2: Example of finite element mesh for mesoscopic unit cell

2. For $j = i$ to n begin:

3. For $s = i$ to n begin:

4. $\overline{\boldsymbol{K}}_{js} = \boldsymbol{K}_{ii}\boldsymbol{K}_{js} - \boldsymbol{K}_{is}\boldsymbol{K}_{ji}$

5. $\overline{\mathbf{F}}_s = \boldsymbol{K}_{ii}\mathbf{F}_s - \boldsymbol{K}_{ji}\mathbf{F}_i$

6. End of loop.

The reduced stiffness matrix then appears in the right bottom corner of the matrix.

When the interior degrees of freedom are eliminated, the multipoint constraints can be applied to the remaining boundary nodes to eliminate the unwanted boundary degrees of freedom. This results in a set of equations

$$\mathbf{q}^B_{meso} = \boldsymbol{T}\mathbf{q}_{macro}, \tag{4}$$

where, see Fig. 2,

$$\mathbf{q}^B_{meso} = \{\mathsf{u}_{11}, \mathsf{v}_{11}, \mathsf{u}_5, \mathsf{v}_5, \ldots \mathsf{u}_{10}, \mathsf{v}_{10}\}^{\mathsf{T}}, \tag{5}$$

$$\mathbf{q}_{macro} = \{\mathsf{u}_{11}, \mathsf{v}_{11}, \mathsf{u}_{12}, \mathsf{v}_{12}, \ldots \mathsf{u}_{14}, \mathsf{v}_{14}\}^{\mathsf{T}}, \tag{6}$$

and $\boldsymbol{T}$ is the transformation matrix representing the way in which the excess boundary degrees of freedom are slaved to the macroelement degrees of freedom. An example of linear interpolation for face 11-14 appears in Fig. 3. In general, however, the master nodes (macroelement boundary nodes) do not have to coincide with the boundary nodes assumed for the mesoscopic finite element mesh. The final stiffness matrix for a given macroelement is obtained by the multiplication of matrices

$$\boldsymbol{K}_{macroelement} = \boldsymbol{T}^{\mathsf{T}}\boldsymbol{K}_{reduc}\boldsymbol{T}. \tag{7}$$

In our particular case the excess boundary degrees of freedom are slaved to the master degrees of freedom employing the Lagrangian interpolation. It means that individual coefficients of the transformation matrix $\boldsymbol{T}$ are obtained as the value of the Lagrangian interpolation function in a given position of the slave node. In particular, consider a one-dimensional regular array of master nodes distributed over the boundary of a 2D domain.

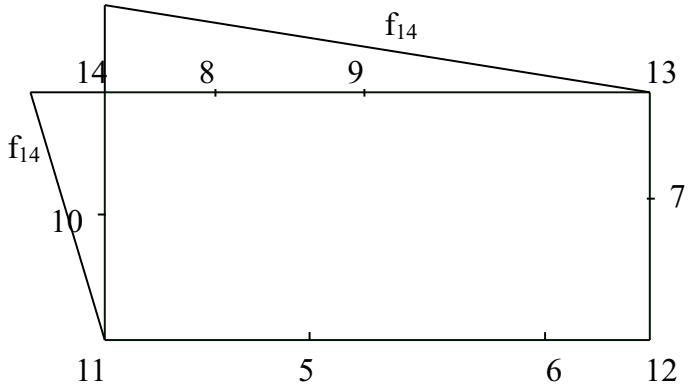

Figure 3: Example of linear interpolation of unwanted boundary nodes for MUC

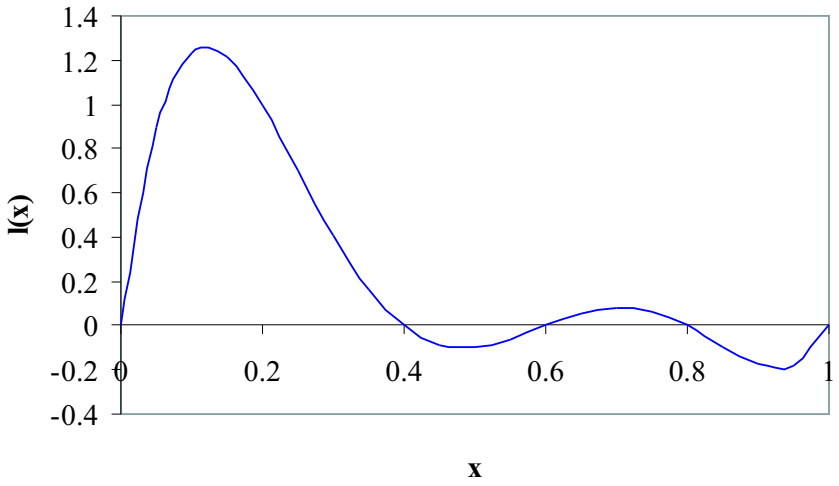

Figure 4: Lagrangian polynomial of the sixth order

Our goal is to find a system of polynomials, where every polynomial has the value 1 for a corresponding master node (its position) and 0 for the others:

$$l_i(x_j) = \delta_{ij}, \tag{8}$$

where x_j is the position of a master node and δ_{ij} is the Kronecker delta; i.e., $\delta_{ij} = 1$ for $i = j$ and $\delta_{ij} = 0$ for $i \neq j$. This condition is fulfilled with the Lagrangian polynomial written as

$$l_j(x) = \frac{(x - x_0)(x - x_1)\dots(x - x_{j-1})(x - x_{j+1})\dots(x - x_n)}{(x_j - x_0)(x_j - x_1)\dots(x_j - x_{j-1})(x_j - x_{j+1})\dots(x_j - x_n)}. \tag{9}$$

An example of such polynomial for one of the six master nodes evenly spread over a given edge of the respective macroelement is plotted in Fig. 4. These polynomials comply with the requirement

$$\sum_i l_i(x) \equiv 1, \tag{10}$$

and so every slave degree of freedom is fully interpolated by all master nodes. In the case of two dimensional array of master nodes (assuming three dimensional mesoscale unit cell

- MUC) the expansion is quite straightforward. In this case the Lagrangian polynomial can be written as

$$l_{ij}(x, y) = l_i(x) l_j(y), \tag{11}$$

where $l_i(x)$ and $l_j(y)$ are the Lagrangian polynomials for the x-axis and y-axis, respectively. Such polynomial again fulfills both conditions (10) and (8).

It should be noted that if the internal degrees of freedom are also slaved to the macroelement degrees of freedom (rather than statically condensed out), a single field approximation is obtained. Finally note that it is not always efficient to order the degree of freedoms such that the Gaussian elimination can be used for obtaining the reduced stiffness matrix and the load vector, since such ordering might result in a large bandwidth.

An alternative approach relies on formal definition of the element stiffness matrix coefficients $\boldsymbol{K}_{ij}$ as

$$\boldsymbol{K}_{ij} = \text{force at dof } i \text{ due to unit displacement at dof } j. \tag{12}$$

Using this definition would simply require a solution of a series of problems in which one degree of freedom is set equal to 1 while the remaining boundary degrees of freedom are fixed. The resulting reaction forces then constitute one column of the reduced stiffness matrix. This process is repeated for each boundary degree of freedom to obtain the entire reduced stiffness matrix. The reduced load vector is obtained by solving one additional problem in which all boundary degrees of freedom are constrained to zero and the internal loads are applied. The negative of the boundary reaction forces then furnish the reduced load vector contribution due to internal loads. Once the reduced set of equations is obtained, the multipoint constraints can be imposed to eliminate the unwanted boundary degrees of freedom. Other more efficient methods were developed to decrease the amount of operations when reducing the stiffness matrix, see, e.g., (Woo and Whitcomb, 1994).

Henceforth, the procedure described above (i.e., static condensation combined with application of multipoint constraints) will be termed “reducing structure”.

3 Coupled analysis

Recall the main objective of this contribution, i.e, the analysis of composite systems with miner difference between individual scales, which makes the direct use of classical, usually uncoupled, homogenization techniques impossible. On the other hand, the use of macroelement within the framework of coupled multiscale analysis is rather straightforward and certainly beneficial from the the solution accuracy point of view when compared to uncoupled approaches. The essential steps governing the coupled multiscale analysis based on macroelement formulation are reviewed in this section.

To make the numerical analysis as accurate as possible the macroscopic finite element mesh is created while taking into account the main geometrical data needed for the construction of the mesoscopic unit cell (the macroelement corner nodes coincide with the vertexes of the mesoscopic unit cell). When material phases on mesoscale experience a nonlinear response, the standard Newton-Raphson method is called to solve the linearized system of macroscopic equations. The macroelement instantaneous (tangent) stiffness matrix and the vector of unbalanced forces follow from the analysis on mesoscale

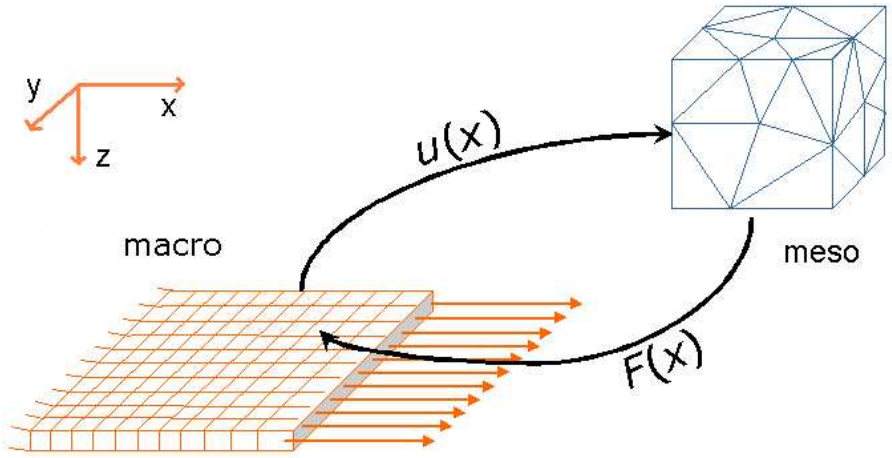

Figure 5: Coupled approach

proceeded by the "reducing structure" procedure. Note that the loading applied on mesoscopic unit cell is provided through master nodes displacement field found from a single macroscopic Newton-Raphson step. Thus for every iteration step the computed macroscopic displacements are transferred to the mesoscale and every macroelement is loaded by these displacements. The reactions from mesoscale nonlinear analysis are transformed back to macroscale and residual forces are computed. The generalized algorithm can be written as, see also Fig. 5,

1. Create mesoscale mesh
2. Reduce this mesh (create macroelement) and compute its stiffness matrix
3. Create macro scale mesh from macro elements
4. Use standard Newton-Raphson analysis
5. For given iteration step i compute macroscale displacements
6. Transform these "macro" displacements into "meso" displacements
7. Load every macroelement by corresponding "meso" displacements
8. Compute "meso" reaction forces for every macroelement
9. Transform "meso" reaction forces into "macro" reaction forces
10. Compute residual forces on macromesh
11. If the error of residual forces is sufficiently small finish the analysis
12. Increase the iteration $i = i + 1$ and go to 5

Clearly, this approach is well suited for parallel computing, where one processor is reserved for macroscale analysis and the remaining processors, if available, perform the analysis on the level of mesoscopic unit cell.

This method is very similar to "brute" force approach but the possibility of parallelization enhanced by the features of error estimation turning off/on the need for mesoscopic analysis can significantly reduce the time needed to complete the analysis.

4 Numerical results

In this section the results of parametric studies using the technique mentioned in the previous section will be summarized. The main goal is to examine an influence of the number of the macroelement nodes on the accuracy of such an element. Four different studies are carried out. The first two are concerned with a 2D model owing to its higher simplicity and the remaining two deal with a 3D model.

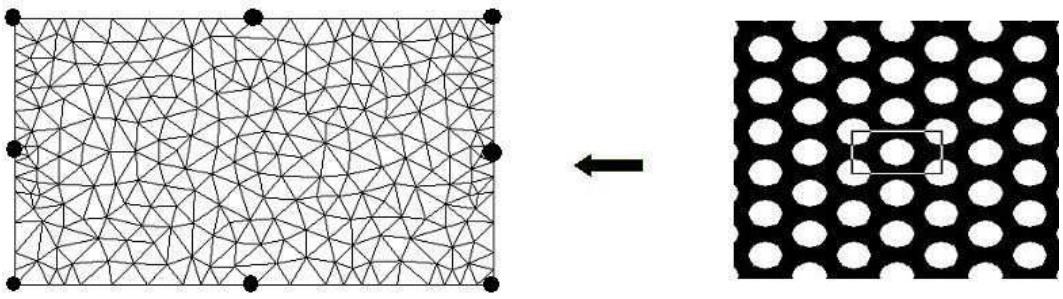

Figure 6: 2D mesh of the mesoscopic unit cell

4.1 2D study

This particular analysis is focused on the influence of the number of boundary nodes being removed purely through *static condensation* (unlike when slaving them to the master nodes via multipoint constrains). A hexagonal packing of carbon fibers embedded in the epoxy matrix is used as a testing two-dimensional example. The macroelement employed for reduced substructuring (highlighted in the center) and the mesh of this mesoscopic unit cell are depicted in Fig. 6. The full mesh has 72 boundary nodes. Five macroelements (i.e., elements with some nodes condensed out) with variable number of boundary nodes are created. In particular, 72, 36, 18, 8 and 4 boundary nodes are preserved after condensation. An example of an 8 node macroelement is plotted in Fig. 6. The selected master (i.e., macro) nodes are represented by small circles. Fig. 7 shows a specific mesh composed of macroelements with 8 nodes. This structure is loaded along one side by the prescribed normal tractions such that the overall sum of the nodal forces remains constant for every type of meshing. The opposite side is fixed. Comparison of average displacement of the loaded nodes including the computational cost appears in Tab. 1 and Fig. 8. Note that the result obtained from 72-nodes macroelement is the exact one (the same as if the full "meso mesh" is used to represent all elements in the entire structure). The results indicate that reducing the number of the boundary nodes through static condensation leads to a considerable error. Condensing out a half of boundary nodes gives approximately 25% error in the displacement field even for a uniform loading. As expected, the time consumption needed for solving the present problem substantially reduces with

the number of nodes being condensed out, but at the expense of the solution error that increases fairly rapidly. The boundary node reduction through static condensation thus does not appear to be appropriate.

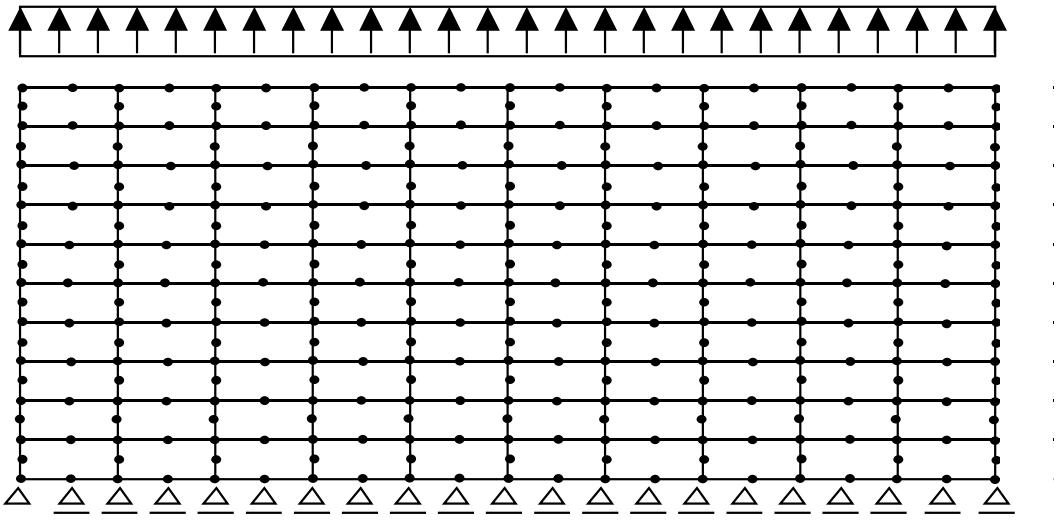

Figure 7: Numerical model from macro elements with 8 nodes

No. of macroelem. nodes	Displacement	Time	Total number of nodes
72	0.0073	146.39	3861
36	0.0085	17.79	1881
18	0.0121	1.69	891
8	0.0244	0.17	341
4	0.0657	0.07	121

Table 1: Comparison of models using reduced substructuring

Next analysis is very similar to the previous one. Again the influence of the number of boundary nodes (i.e., nodes of macroelement), which will remain after "reducing structure" step, is examined. The geometrical model of the reduced structure is shown in Fig. 6. Again this model has 72 boundary nodes. Unlike the first study, only the inner nodes of this model are condensed out. The excess boundary nodes are then reduced by the *multipoint constraints*. In our particular case only the linear interpolation for slaving the boundary degrees of freedom of mesoscopic unit cell to macroelement master nodes (it can be imagine as the Lagrangian polynomial with only two lateral master nodes) was used. Nevertheless, the quadratic interpolation was tested too, but the resulting stiffness matrices derived for both linear and quadratic interpolation were fairly similar and thus the quadratic interpolation was left out for further analysis. With reference to the previous example, the same finite element mesh, Fig. 7, together with the same loading conditions was assumed.

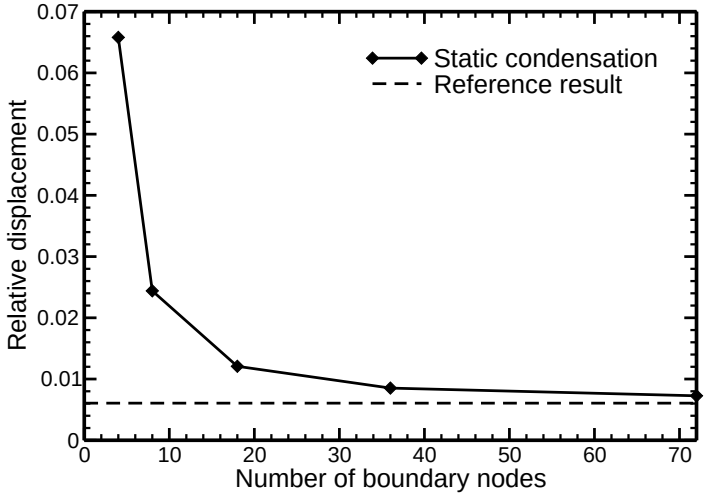

Figure 8: Comparison of relative displacements

No. of macroelem. nodes	Displacement	Total number of nodes
72	0.00735	3861
36	0.00733	1881
18	0.00728	891
8	0.00710	341
4	0.00712	121

Table 2: Comparison of models using static condensation with linear interpolation constraints

The resulting average displacement of the loaded nodes for individual cases of the degree of unwanted boundary dofs removal are stored in Tab. 2. Clearly, the results are much more accurate in comparison with the previous example. The error for the 4-node macroelement is only 3%. It means that the boundary degrees of freedom must not be eliminated by static condensation but rather with the help of multipoint constraints.

4.2 3D study

To confirm individual conclusions drawn from two dimensional study a three dimensional analysis is explored in this section. Two specific examples are addressed. First, an artificial problem of plate consisting of a set of cubic mesoscopic unit cells is considered to examine the influence of mesh density of a unit cell and the degree of boundary nodes reduction on the solution accuracy. Second example is devoted to the application of proposed approach to the macroscopic analysis of wound composite tube, where, owing to the complicated geometry, the coupled multiscale analysis employing the macroelement formulation seems to be the only option.

In view of the previous results the static condensation combined with multipoint constrains is used exclusively starting with the influence of mesh refinement on the level of

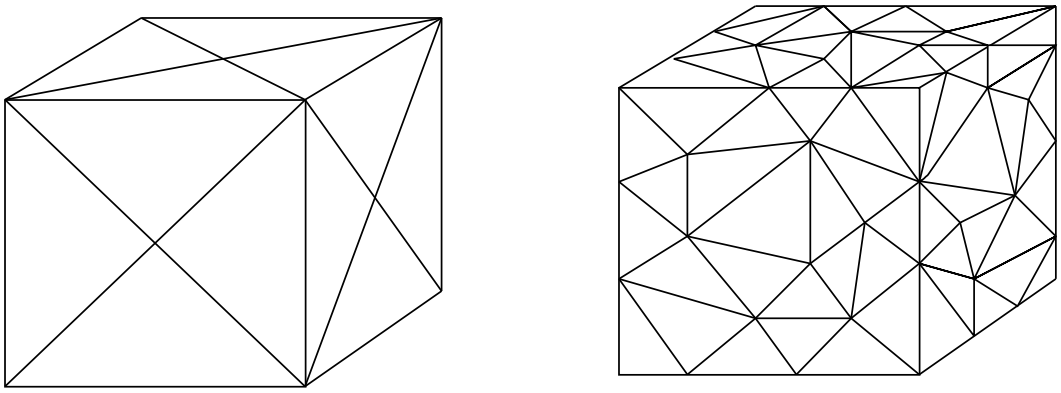

Figure 9: Example of fine and coarse MUC mesh

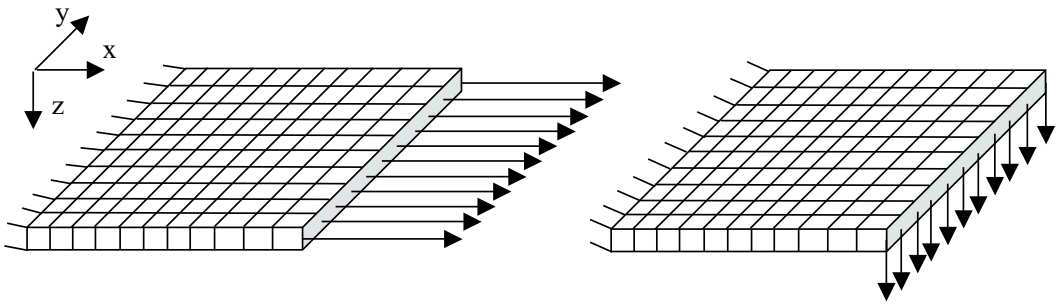

Figure 10: Loading of plate (in-plane loading and out-of-plane loading)

unit cell. To that end, consider a cubic mesoscopic unit cell of Fig. 9. Six meshes of various degree of refinement were tested, see Fig. 9 for an example of coarse and fine mesh. For each mesh the macroelement is derived by condensing out all inner degrees of freedom and then introducing multipoint constrains to arrive at 8-node brick macroelement (bilinear interpolation is used for tying the master and slave nodes). This element is then used in macroscale analysis assuming plate of 10×10 elements loaded by in-plane and out-of-plane forces according to Fig. 10. The results represented by displacements developed along the loaded edge appear in Tab. 3. Clearly, refining the finite element mesh produces more compliant results. As expected, for in-plane loading the effect of mesh refinement is rather inferior while for out-of-plane loading an error with respect to the finest mesh is about 23%. These results are only qualitative as no "exact" solution is available. Also note that for each unit cell the transversally isotropic material with the plane of isotropy normal to the direction of in-plane loading was selected.

More interesting results follow from studying the effect of the boundary degrees of freedom reduction. A cubic mesoscopic unit cell with 11 nodes along each edge is assumed. For the purpose of removing the unwanted boundary degrees of freedom several macroelements with evenly distributed master nodes along individual edges were developed. Note that their locations do not correspond to the original unit cell boundary nodes locations. The Lagrangian polynomials are therefore used for interpolation. Elements with 2 to 12 master nodes along the edge were considered. The loading was limited to uniform in-plane tractions only, i.e., the sum of all node loads was equal for every macroelement.

The results in terms of the axial displacements developed along the loaded edge are plotted in Fig. 11. The number in figure legend represents the overall number of master

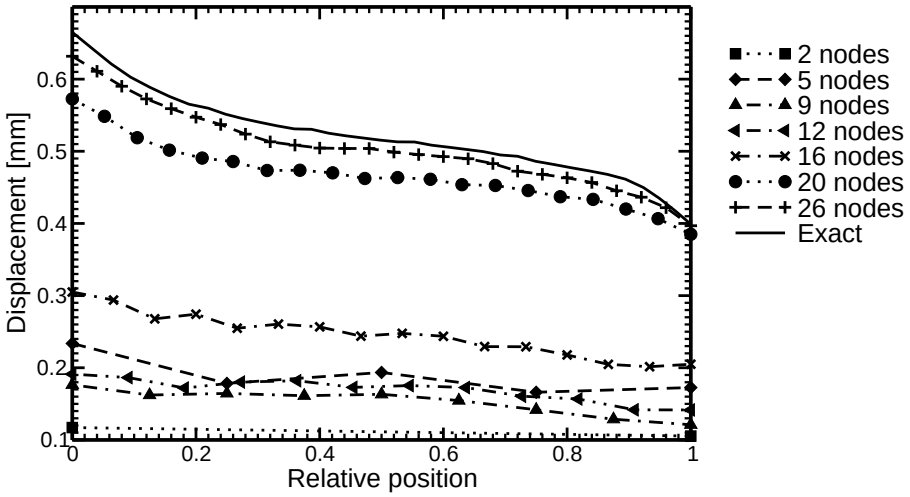

Figure 11: Displacements along the loaded edge

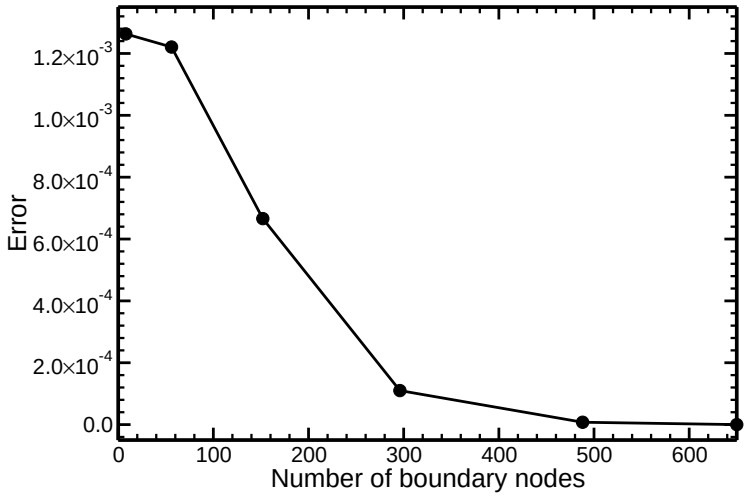

Figure 12: The error in displacements along the loaded edge

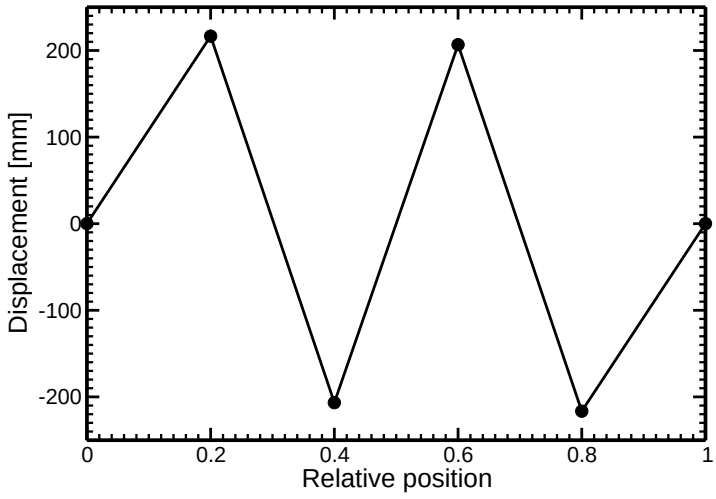

Figure 13: Tensile displacements along the loaded edge assuming 12 master nodes per edge of a cube

mesh	1	2	3	4	5	6
No.of nodes	1515	199	68	42	20	13
in-plane l. u_x [mm]	0.2067	0.2062	0.2056	0.2064	0.2029	0.2027
in-plane l. u_z [mm]	0.0053	0.0054	0.0063	0.012	0.0052	0.0058
out-of-plane l. u_z [mm]	57.25	54.96	51.09	48.53	45.7	44.4

Table 3: Results for in-plane and out-of-plane loading

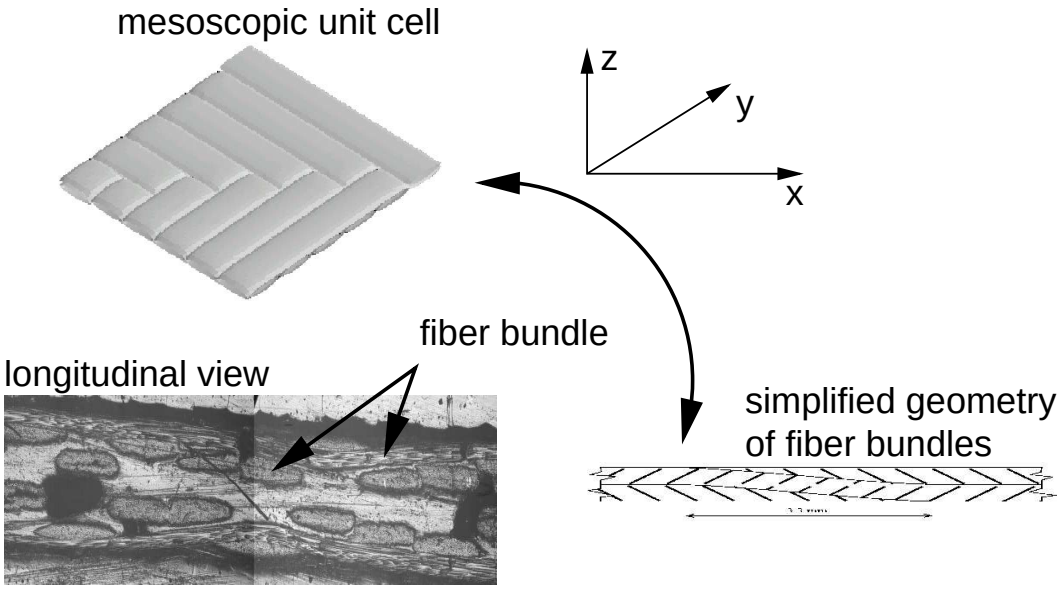

Figure 14: MUC and longitudinal view of a section of real composite tube.

nodes along the edge. The exact solution is derived from the macroelement, where only the inner nodes are condensed out. Fig. 12 shows the relative error computed as the L_2 norm of a difference of the displacements along the loaded edge, Fig. 11, with respect to the "exact" solution. Note that the accuracy of the results depends on the number of master nodes more significantly than in 2D analysis. While for 3 nodes per edge the error exceeds 0.001, for 10 nodes the error is only 7×10^{-6}. It is interesting to note that number of master nodes exceeding the number of boundary nodes of the original unit cell provides rather oscillatory behavior as evident from Fig. 13 displaying oscillation of the displacements for 12 master nodes along the macroelement edge. This can be attributed to the fact that the size of the macroelement stiffness matrix is larger than the matrix obtained just by condensing out all inner degrees of freedom. It means that some additional degrees of freedom are added leading to an "unstable" structure.

The final example is devoted to the wound composite tube. The geometry of the mesoscopic unit cell, its cross-section together with a real micrograph are shown in Fig. 14. In this example, only a single macroelement resulting from the "structure reducing" step applied to the mesoscopic unit cell of Fig. 14 is examined with respect to the effect of removal of unwanted boundary degrees of freedom. As for the boundary conditions, one side of the MUC was fixed while the opposite side was subjected to tensile uniform

tractions. As in the previous examples the overall loading is kept constant for every macroelement. Fig. 15 shows evolution of the tensile displacements along the upper loaded edge of the unit cell of woven composite. The number in the legend stands again for the number of master nodes placed along the edge of a given macroelement. Clearly, the error for small number of master nodes is quite significant. For further evidence, see Fig. 16. Note that for 5 nodes per edge the error is about 0.17 in L_2 norm, while for 28 nodes the error drops down to 0.005. In the latter case the number of nodes in macroelement reduces to 1626 nodes compared to 2432 nodes for macroelement derived from pure condensation ("exact solution").

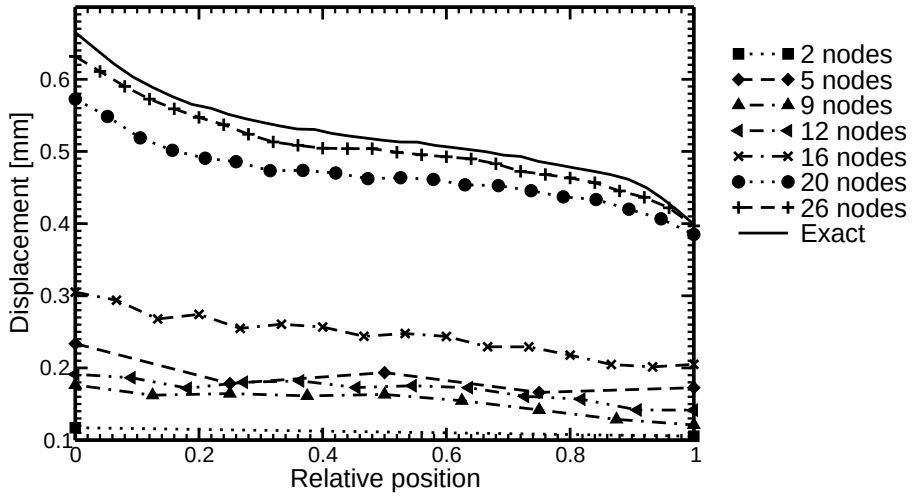

Figure 15: Tensile displacements along the loaded upper edge of the MUC

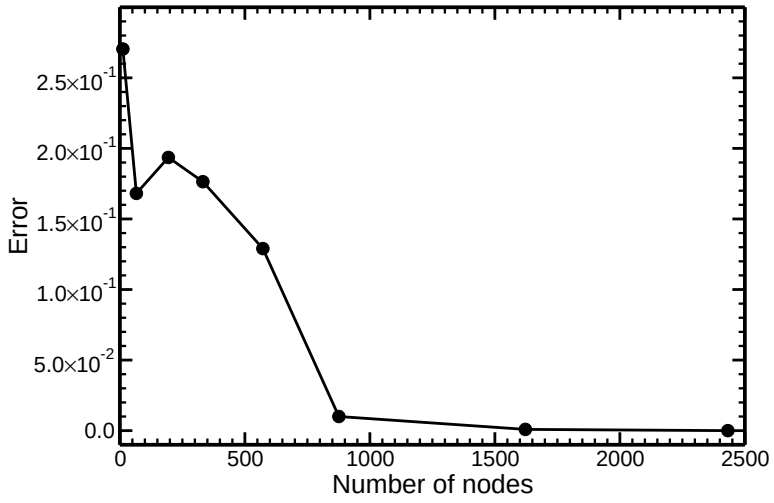

Figure 16: The error in displacements along the MUC edge

Unfortunately, the static condensation itself brings for the present unit cell only a minor reduction in the overall number of degrees of freedom. This is attributed to the fact that there are only two elements placed over the MUC thickness, thus the ratio between the number of boundary nodes and the overall number of nodes of the mesoscopic unit cell is quite small and so the reduction of this structure is not so efficient. Finally, as in the case cubic unit cell, if the number of master nodes in some direction is higher then

the real number of boundary nodes the displacements start to oscillate and the results are meaningless.

5 Conclusion

The formulation of macroelement based on the static condensation is described in the paper. This method begins with the formulation of mesoscopic global stiffness matrix followed by static condensation of inner degrees of freedom from the mesoscopic finite element mesh. Finally, a set of constraints is applied to eliminate the unwanted boundary degrees of freedom (slaving the selected set of boundary degrees of freedom of a MUC to master nodes of a given macroelement). This procedure results into a macroelement having a representative structural stiffness matrix, which can be directly used in the macroscale analysis. The advantage of this method is that there is direct coupling between meso and macroscale through macroelements. The results show that static condensation applied also to boundary degrees of freedom leads to erroneous results. Therefore, the proper procedure of eliminating the unwanted boundary degrees of freedom corresponds to the application of multipoint constraints. Application of "structure reducing" step to rather flat MUC such the wound composite tube is not very beneficial since the resulting macroelement, in order to have a tolerable accuracy, must contain a significant number of nodes so that its use on the macro level is not that efficient. Nevertheless, in case of "reasonable" mesoscopic unit cells the reduction of the number of nodes (degrees of freedom) is quite high and so it allows for substantial savings in the computational time.

Acknowledgments

This support provided by the GAČR No. 106/03/H150 and CEZ MSM 6840770003 is gratefully acknowledged.

References

Fish, J. (1992). Hierarchical modelling of discontinuous fields. *Commun. Appl. Numer. Methods*, 8:443–453.

Fish, J., Shek, K., Pandheeradi, M., and Shephard, M. S. (1997). Computational plasticity for composite structures based on mathematical homogenization: Theory and practice. *Computer Methods in Applied Mechanics and Engineering*, 148(1–2):53–73.

Fish, J., Yu, Q., and Shek, K. (1999). Computational damage mechanics for composite materials based on mathematical homogenization. *International Journal for Numerical Methods in Engineering*, 45(11):1657–1679.

Foye, R. L. (1988). The mechanics of fabric reinforced composites. In *Proceedings of fiber-tex conference*, pages 237–247.

Kamel, H., Liu, D., McCabe, M., and Phillipopoulos, V. (1972). Some developments in the analysis of complex ship structures. *Advances in computational methods in structural mechanics and design*, pages 703–726.

Kouznetsova, V., Geers, M. G. D., and Brekelmans, W. A. M. (2002). Multi-scale constitutive modelling of heterogeneous materials with a gradient-enhanced computational homogenization scheme. *International Journal for Numerical Methods in Engineering*, 54(8):1235–1260.

Šejnoha, M. (1999). *Micromechanical analysis of unidirectional fibrous composite plies and laminates*, volume 3 of *CTU Reports*. Czech Technical University in Prague.

Whitcomb, J., Woo, K. S., and Gundapaneni, S. (1994). Macro finite-element for analysis of textile composites. *Journal of Composite Materials*, 28(7):607–618.

Wierer, M. (2005). *Multi scale analysis of woven composites*. PhD thesis, Faculty of Civil Engineering, Czech Technical University in Prague.

Woo, K. and Whitcomb, J. (1992). Macro finite element using subdomain integration. In *OTRC Report*, Texas, A&M University.

Woo, K. and Whitcomb, J. (1994). Enhanced direct stiffness method for finite element analysis of textile composites. *Composite structures*, 28:385–390.

Zeman, J. (2003). *Analysis of Composite Materials with Random Microstructure*. PhD thesis, Czech Technical University, Prague.

Keywords: Macroelement, multiscale modeling, static condensation, multipoint constraints, mesoscopic unit cell (MUC)

List of Figures

List of Tables